crystals

MDPI

Article

Structural Properties of Yttrium Aluminum Garnet, Doped with Lanthanum

Nurgul Zhanturina [1,*], Daulet Sergeyev [2], Zukhra Aimaganbetova [1], Abzal Zhubaev [1] and Karlygash Bizhanova [3]

[1] Department of Physics, K.Zhubanov Aktobe Regional University, Aktobe 030000, Kazakhstan
[2] Scientific Center "Radiation Physics of Materials", K.Zhubanov Aktobe Regional University, Aktobe 030000, Kazakhstan
[3] Department of Fundamental Sciences, Yessenov University, Aktau 130000, Kazakhstan
* Correspondence: zhanturina_n@zhubanov.edu.kz; Tel.: +7-7013684899

Abstract: The results from simulation of the structural and optical properties of YAG pure, doped with two ions and four ions of lanthanum, are presented in this paper to investigate the effect of dopants on a crystal. The simulation was carried out in the Quantum Espresso program. The band structure, density of states, the dielectric function, absorption, refractive index, energy loss function and reflectivity were calculated for different samples. It can be assumed that with a rise in concentration density of states, the impurity atom increases and the position of the most populated levels shifts to the right in the region of negative energies in the case of two atoms and to the left in the case of four atoms of lanthanum. We can draw conclusions about the transparency of the sample in the visible region, because the absorption spectra appear in the UV region. This transparent nature makes them perfect candidates for deep UV nonlinear optical materials. From the analysis of dielectric function, it is clear that in the case of YAG doped with two ions of lanthanum, two peaks appeared compared to the sample with one peak in pure and doped with four ions. Anisotropy is most pronounced with an increase in the degree of doping.

Keywords: garnet; lanthanum; density functional theory; dielectric function; absorption

Citation: Zhanturina, N.; Sergeyev, D.; Aimaganbetova, Z.; Zhubaev, A.; Bizhanova, K. Structural Properties of Yttrium Aluminum Garnet, Doped with Lanthanum. *Crystals* **2022**, *12*, 1132. https://doi.org/10.3390/cryst12081132

Academic Editors: Yuui Yokota and Takahiko Horiai

Received: 14 July 2022
Accepted: 9 August 2022
Published: 12 August 2022

1. Introduction

Garnets and perovskites, orthosilicates and phosphates doped with Ln ions are known as scintillator and phosphor materials, especially due to the short lifetime (high emission rate) of the luminescence [1–3]. Doped with other transition elements, such as Nd, Pr or Mn, they have many other important applications, for instance, as solid-state laser materials [4,5], thermoluminescence dosimeters [6,7], thermometers etc.

One of the urgent problems in modern optoelectronics and the chemistry of optical materials is the search for new materials with outstanding physicochemical properties [8]. Yttrium aluminum garnet (YAG) is considered the most-studied compound in the garnet class. In the development and application of "white light" LEDs, cerium-doped yttrium-aluminum garnet (YAG:Ce) nanopowders are among the most important phosphors, since YAG:Ce^{3+} nanopowders are suitable for converting blue LED radiation into broadband yellow light. The quality of YAG:Ce phosphors, such as purity and particle size, affect the brightness and efficiency of white LEDs. The synthesis of high-quality YAG:Ce phosphors is important. Various white mixtures are the basis for the manufacture of phosphors for LEDs.

Yttrium aluminum garnet, $Y_3Al_5O_{12}$ (YAG) single crystals, doped with rare-earth ions (e.g., Nd^{3+} and Yb^{3+}), is widely used as active laser media in solid-state lasers [9].

Yttrium aluminum garnet (YAG, $Y_3Al_5O_{12}$) is a synthetic crystalline material in the garnet group. YAG, like a pomegranate and sapphire, is not used as a laser medium in its pure form. However, after doping with the corresponding YAG ion, usually, it is used as a host material in various solid-state lasers. In an elementary cell of yttrium garnet, there are

eight $Y_3Al_5O_{12}$ molecules, a total of 24 yttrium ions, 40 aluminum ions and 96 oxygen ions. When the material is doped with rare-earth ions, they replace yttrium.

Many researchers have studied the properties of pure and substituted YAG [10–12]. It should be noted that, in general, many works are devoted to studies of the spectroscopic characteristics of crystals, strained or doped, with different concentrations of defects. Modeling crystals with various impurities and varying degrees of concentration in order to obtain materials with desired properties is very promising and relevant. In the synthesis of certain materials, the optical properties are determined immediately after their preparation, especially since the process of solid-phase synthesis requires time, resources and consumables. The first principles in this case are comparative studies of the band structure and optical properties of yttrium garnet doped with rare-earth ions in different concentrations.

In the investigation of optical properties of materials, modeling of the energetic structure of the phosphors and spectroscopic characterization of the phosphor materials are very important. For the simulation of properties the wavefunctions based on ab initio quantum chemistry, methods will be used in order to determine the electronic structure of ground and excited states of lanthanide and transition metal-doped crystals. In the literature, the results on the experimental spectroscopic data of yttrium garnet doped with cerium and praseodymium are quite widespread [13]. However, data on doping with lanthanum would be very interesting, since in the literature, studied by us, there were no results regarding data on the study of the optical properties of these objects. Lanthanum is of special interest among rare-earth elements. The presence of lanthanum impurity in the initial alumina matrix, as well as of many other earth elements, leads to the formation of new centers with unique properties [14,15]. The lanthanum impurity can efficiently localize low-energy excitations (electrons, holes and excitons) owing to the non-Coulomb potential during a nucleus cation substitution [16]. La is the second-most-abundant rare-earth metal after cerium. It is mostly used in optical glasses, rechargeable batteries due to its ability of hydrogen storage and catalysts [17].

Lanthanum has other dopant properties than lanthanides because it has no 4f transition. Due to this fact, it is relevant to examine the electric properties, light-absorption properties and simple band structure of this material. To the best of our knowledge, only very few works have been reported in detail in the literature on La-modified YAGs.

Observation of dielectric properties of this material may be useful for device applications of microwave absorbers. The enhancement in multiferroic properties suggests a potential application in multiferroic devices [18]. Multiferroic materials are very unique due to the coexistence of both ferroelectricity and ferromagnetism and are being extensively investigated by researchers worldwide due to their potential applications in novel devices, such as sensors, actuators, storage information, spintronics and microelectronic devices [19,20].

To predict the properties in yttrium garnet phosphors doped by lanthanum in different concentrations, the ab initio calculations helps us. Let us review the ab initio modeling of the band structure and optical characteristics in yttrium garnets. In [21], various charged vacancies in yttrium aluminum garnet ($Y_3Al_5O_{12}$) were studied using the ab initio method. The local atomic structures, electronic structure, defect states and formation energies of vacancies are calculated. The optical transition induced by an oxygen vacancy is predicted and the stability of the charged oxygen vacancy is discussed.

In [22], the 4f↔5d absorption and emission spectra of Ce^{3+} doped YAG ($Y_3Al_5O_{12}$) are simulated with a quantum chemical ab initio embedded cluster approach, applied to Ce^{3+} substitutional defects in D_2 local symmetry. The simulated absorption spectrum is calculated with overestimations of 2300–3300 cm^{-1}, which became 4600 cm^{-1} in the luminescence. Good absorption and emission band shapes and relative intensities are obtained. A large underestimation of the Stokes shift is found, which suggests an underestimation of the relaxation on the emitting state.

In this paper, we present a series of first-principles density function theory calculations on the band structure, density of states and dielectric function calculations for the pure

sample and that doped by lanthanum in different concentrations of yttrium garnet, as a first and necessary step towards the future investigation of the effect of defects in a crystal. The doping with two ions and four ions of La was used to examine the changes in band structure, absorption properties and dielectric properties of material to obtain a sample with the desired properties.

2. Materials and Methods

The simulation was carried out in the Quantum Espresso program 6.7 (Italy). The Quantum Espresso package is a multi-purpose and multi-platform software for ab initio calculations of condensed matter (periodic and disordered) systems. Codes in the package are based on density functional theory and on a plane wave/pseudopotential description of the electronic ground state and are ideally suited for structural optimizations (both at zero and at finite temperature), linear response calculations (phonons, elastic constants, dielectric and Raman tensors, etc.) and high-temperature molecular dynamics. The studies were carried out using three samples: pure yttrium garnet $Y_3Al_5O_{12}$, yttrium garnet doped with two lanthanum ions, also four. Geometry optimization was conducted in Atomistic Toolkit with Virtual Nanolab 15.1 (Synopsis, Copenhagen, Denmark) (ATK VNL). ATK VNL is a leading industry-proven platform for atomic-scale modeling of materials, nanostructures and nanoelectronic devices. It includes quantum mechanical methods such as density functional theory (DFT) with either LCAO or plane-wave basis sets and semiempirical models, simulation engine for atomic-scale simulations using classical potentials, module for nanoscale device and transport simulations using non-equilibrium Green's function (NEGF) methodology.

The crystal structure contains dodecahedral (8 vertices), octahedral (6 vertices) and tetrahedral (4 vertices) positions. The elementary cell contains eight formula units and includes 24 dodecahedral positions of Y, 16 octahedral positions of Al(1) and 24 tetrahedral of Al(2) and 96 positions of O. When the material is doped with rare-earth ions, they replace yttrium. The optimized lattice constants are shown in Figure 1.

The simulation consists of the following sequential steps. First, the geometry of the molecule is optimized. At this stage, the atomic composition of the molecule is established and the equilibrium interatomic bonds are calculated, which correspond to the minimum energy.

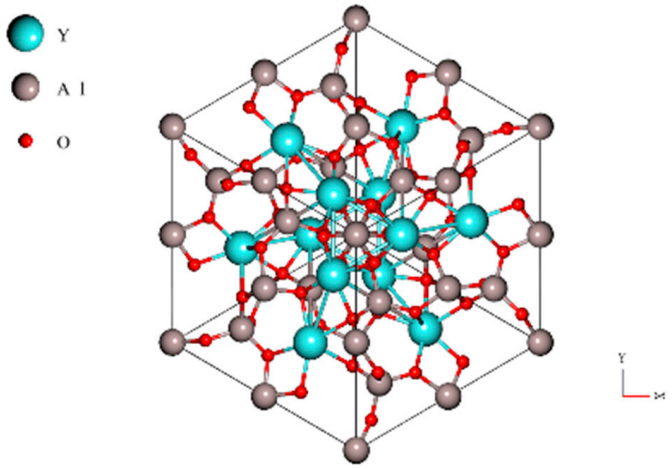

(**a**)

Figure 1. *Cont.*

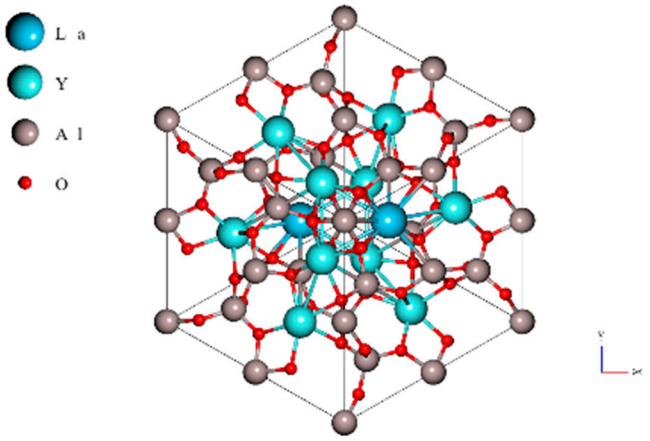

(**b**)

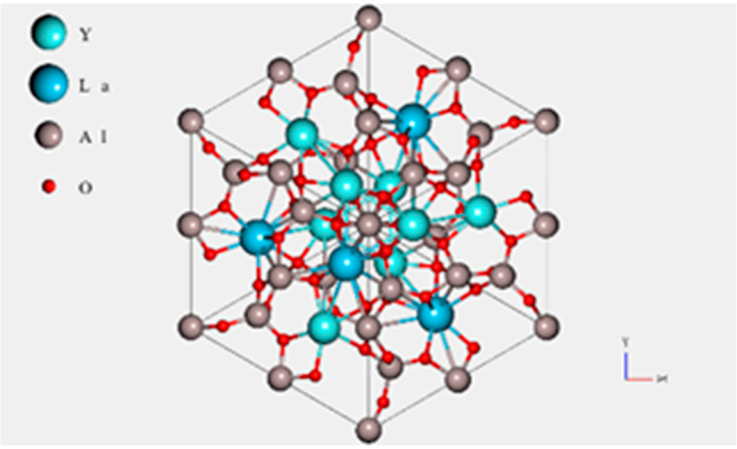

(**c**)

Figure 1. Elementary lattices of $Y_3Al_5O_{12}$: (**a**) $Y_3Al_5O_{12}$; (**b**) $Y_3Al_5O_{12}$:La (2 ions); (**c**) $Y_3Al_5O_{12}$:La (4 ions).

The optical characteristics of $Y_3Al_5O_{12}$:La were simulated using the Quantum EPRESSO software package. The procedure for optimizing the geometry of the structure under consideration and describing the interatomic interaction was carried out in the framework of the density functional theory (DFT); the generalized gradient approximation GGA-PBE was used as the exchange-correlation functional. When optimizing the structures, the parameters of the atomic configuration relaxed until the forces on all atoms became less than the specified threshold value of 0.02 eV/Å. The introduction of the La impurity was carried out by replacing the Al atom with the La atom near the center of the supercell, followed by the relaxation of all atoms.

Computer simulation of the optical characteristics of $Y_3Al_5O_{12}$; $Y_3Al_5O_{12}$:La was produced within the framework of DFT-GGA using the Kubo–Greenwood equation, which determines their dielectric susceptibility:

$$\chi_{ij}(\omega) = -\frac{e^2\hbar^4}{m_e^2\varepsilon_0 V\omega^2}\sum_{nm}\frac{f(E_m)-f(E_n)}{E_{nm}-\hbar\omega-i\hbar\Gamma}\pi^i_{nm}\pi^j_{mn} \quad (1)$$

where π^i_{nm} is component of the dipole matrix element between state n and m, V the volume, Γ the broadening and $f(E)$ Fermi function, e is the charge of the electron, $\hbar$ is Planck's constant, E is energy, $f(E)$ is the Fermi distribution function of quasiparticle energy, ε_0

dielectric permittivity of vacuum, ω frequency and m_e electron's mass. From Equation (1), the dependence of the permittivity on frequency (on energy) is determined:

$$\varepsilon(\omega) = 1 + \chi(\omega) \tag{2}$$

Using the imaginary and real parts of the permittivity (2) we find the extinction coefficient:

$$k(\omega) = \sqrt{\frac{\sqrt{\mathrm{Re}(\varepsilon)^2 + \mathrm{Im}(\varepsilon)^2} - \mathrm{Re}(\varepsilon)}{2}} \tag{3}$$

From (3) the optical absorption coefficient is determined:

$$\alpha = 2\frac{\omega}{c}k \tag{4}$$

3. Results

3.1. Band Structure

The band structures and total density of states calculations show that the bottom of the conduction band and the top of the valence band occurred at the Γ point, indicating a direct band gap in value around 4.7 eV in poor crystal as it can be seen from Figure 2. This value is smaller than the experimental band gap of 6.3 eV in pure yttrium garnet [23,24]. The bandgap is 4 eV in crystal with two La ions and the same bandgap with four La Ions. The difference between latter structures in the fact that the conduction band starts from 1 eV in the sample with two La and from 2 eV with four La. The difference between the two samples in the fact that in the sample doped with two La ions, the conduction band starts from 1 eV, four La ions from 2 eV.

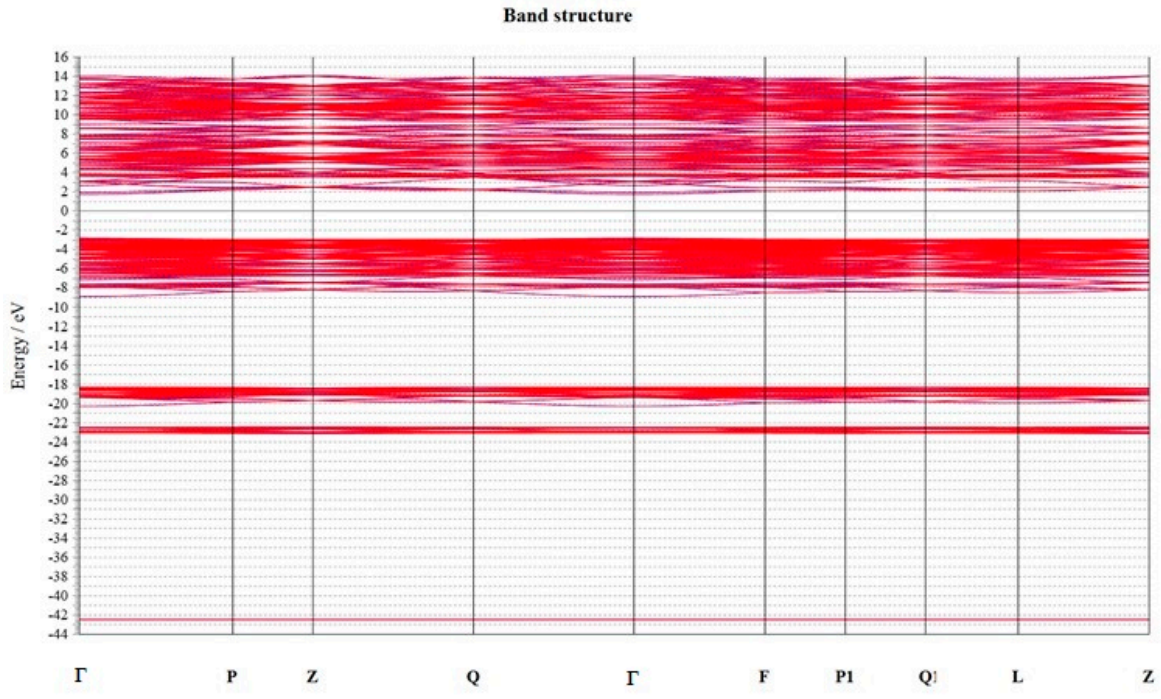

(**a**)

Figure 2. *Cont.*

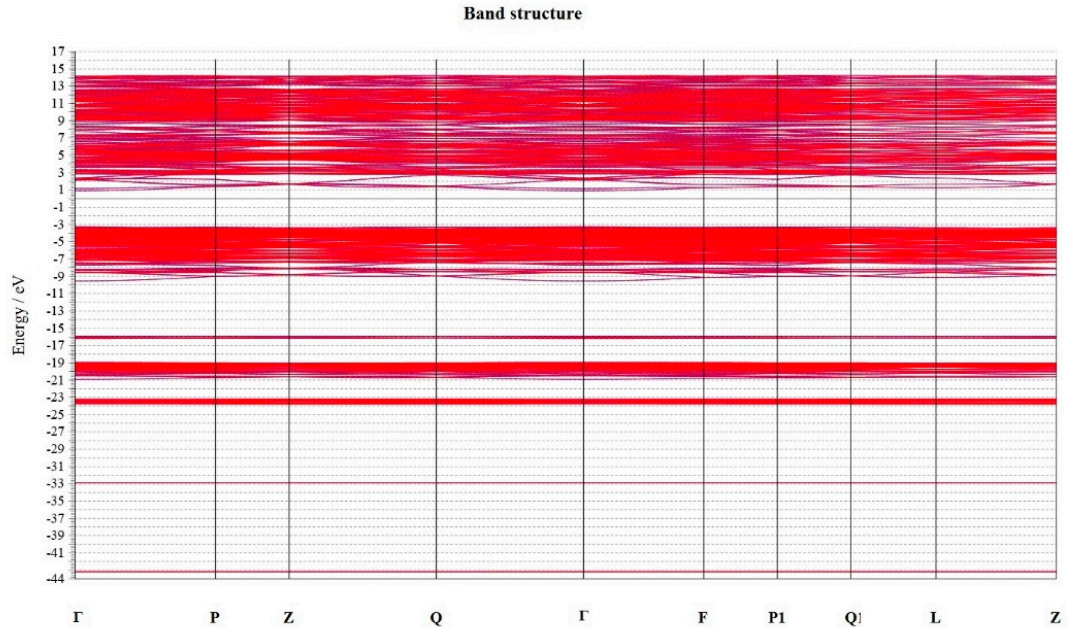

(**b**)

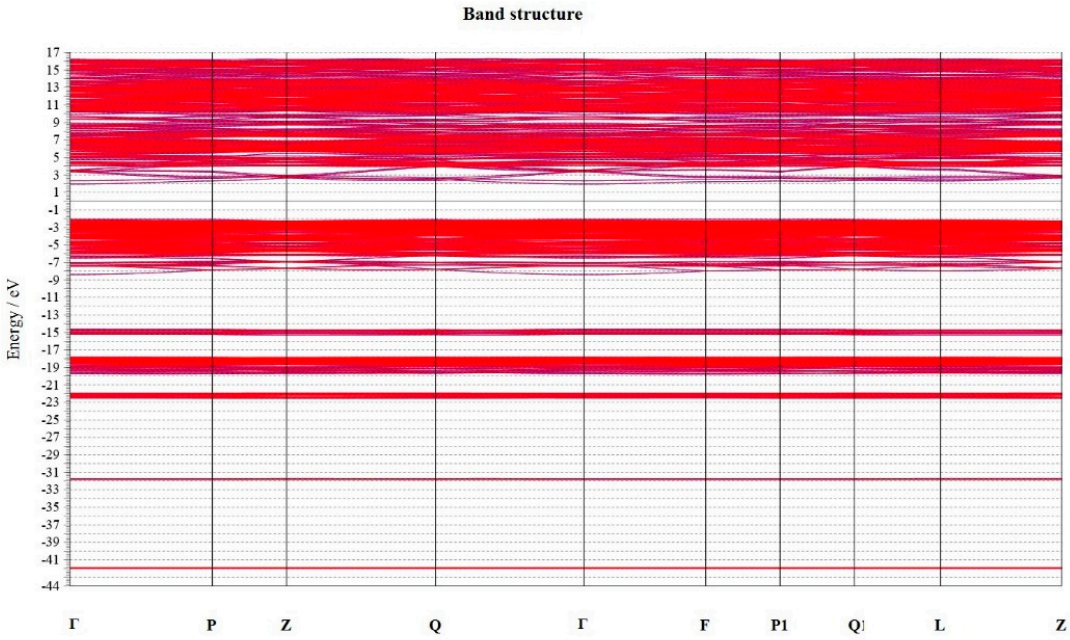

(**c**)

Figure 2. Band structure of the samples (**a**) $Y_3Al_5O_{12}$, (**b**) $Y_3Al_5O_{12}$:La (2 ions), (**c**) $Y_3Al_5O_{12}$:La (4 ions).

3.2. Density of States

In Figure 3, the density of electronic states as a function of energy for three types of geometry is shown. In all cases, the Fermi energy in the systems is reduced to zero.

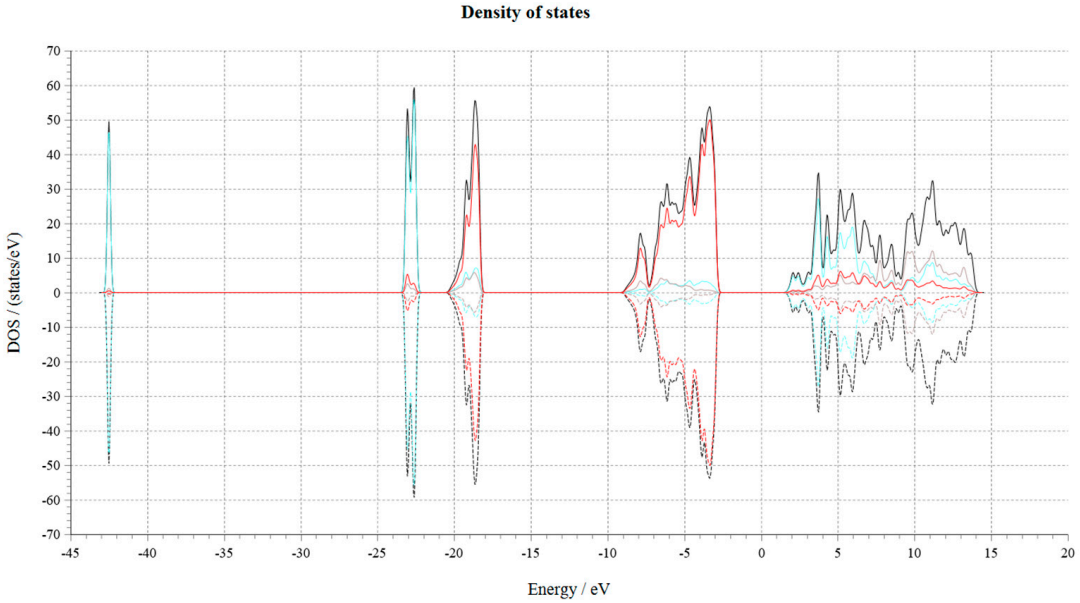

(**a**)

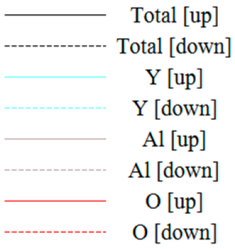

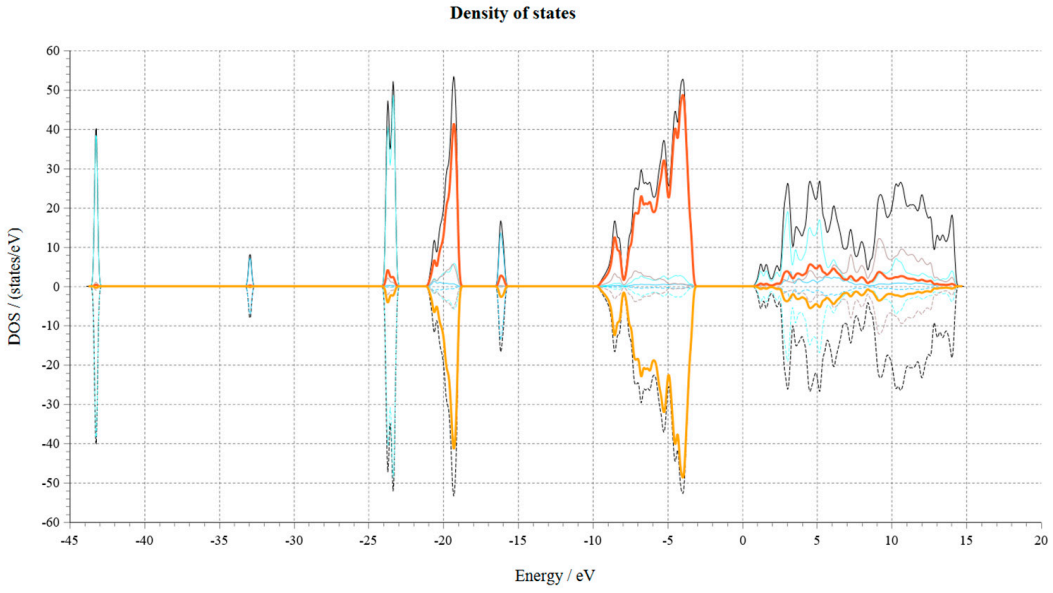

(**b**)

Figure 3. *Cont.*

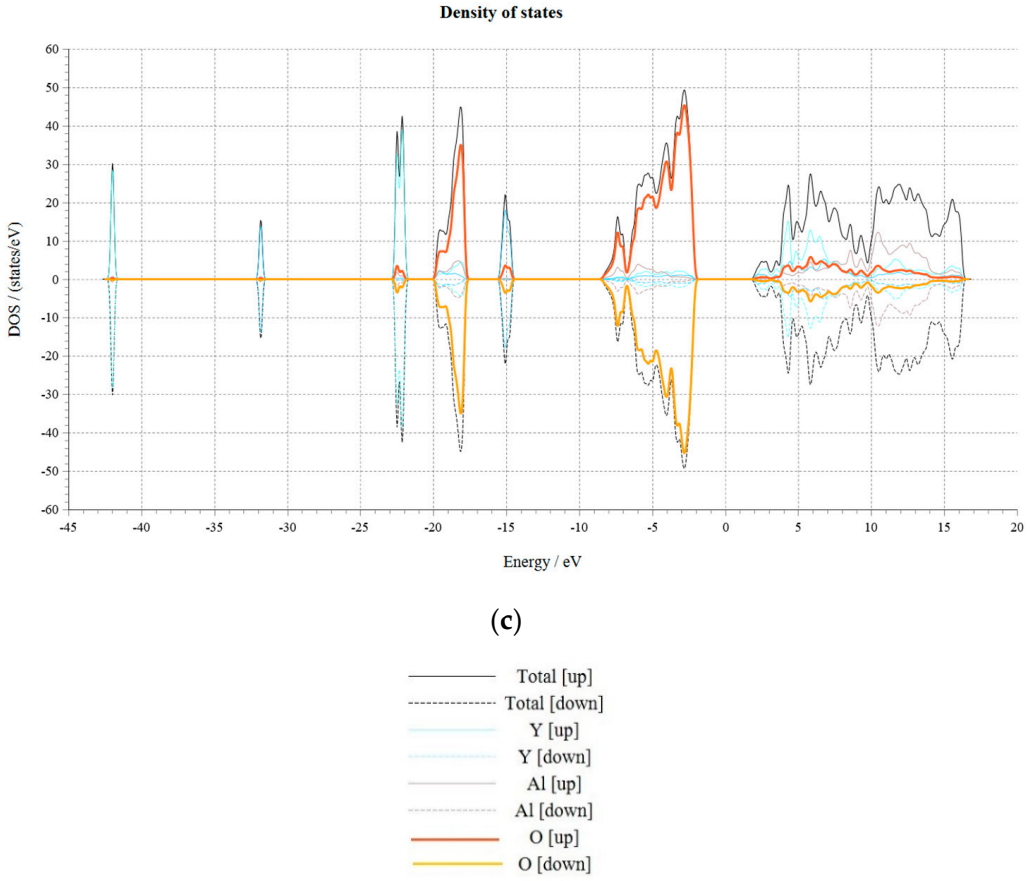

Figure 3. Density of states (**a**) $Y_3Al_5O_{12}$, (**b**) $Y_3Al_5O_{12}$:La (2 ions), (**c**) $Y_3Al_5O_{12}$:La (4 ions).

In Figure 3, the total and partial density of states are presented. "[Up]" and "[down]" mean the positive and negative DOS, respectively. Black lines correspond to the total density of states and other lines are due to the partial DOS of yttrium, aluminum and oxygen, according to the figure legends. The range of negative energies corresponds to filled molecular orbitals, and to positive ones, unfilled ones. The band gap corresponds to the left boundary of states in the region of positive energies. In the case of pure yttrium garnet, it can be seen that the most populated are levels with energies of about −23 eV and 19 eV; there are absolutely no states in a range from −42.5 eV to −23 eV and −19 eV to −9 eV.

The low valence bands in a range of −23 to −19 eV are contributed by O-s states and minor contribution of Y-d and Al-d states. The upper valence bands in a range of −9 to −3 eV are mainly composed of O-p states, hybridized with some Al-3d and Y-3d electrons. The conduction band is predominantly occupied by Y-3d, Al-3d and O-2p electrons.

Geometry optimization within the ATK VNL method and the starting distorted geometry give an approximately equal and less accurate value of 4.3 eV. It should be noted that, when calculating using the density functional theory, taking into account only local correlations, even within a sufficiently accurate approximation, the value of the energy for the lower unfilled state is determined with a systematic error due to the limitation of the theory [25].

In the case of doping with two Lanthanum atoms, the most occupied states shift slightly to the left in the region of negative energies and the population decreases in comparison with the pure sample; the band gap decreases to 4 eV. Population of the −32.5 eV, −16.5 energy level is associated with lanthanum appearing. When the concentration increases to four Lanthanum atoms, the DOS at these energies increases.

It can be noted that, with an increase in the number of doped atoms, the DOS in the most populated levels of the host decreases and DOS in the impurity atom increases

and the position of the most populated levels shifts to the left in the region of negative energies in the case of two atoms and to the right in the case of four atoms. For small impurity concentrations, implying negligible interaction between impurity atoms, the energy dependence of the impurity states is adequately described by a delta function. As the impurity concentration increases, interaction begins to become important and the (spatially averaged) density of impurity states begins to spread; most of the states still reside at the nondegenerate level and the spread occurs around this energy [26]. Therefore, at high concentrations, the impurity level spreads into the impurity band, overlapping with the conduction band.

3.2.1. Optical Properties of Pure Yttrium Garnet

The imaginary and real parts of the dielectric function are presented in Figures 4–7. On the insert to figures "Imxx", "Imyy", "Imzz", "Rexx", "Reyy" and "Rezz" mean the imaginary (Im) and real (Re) part of dielectric function by the *X*, *Y* and *Z* axis.

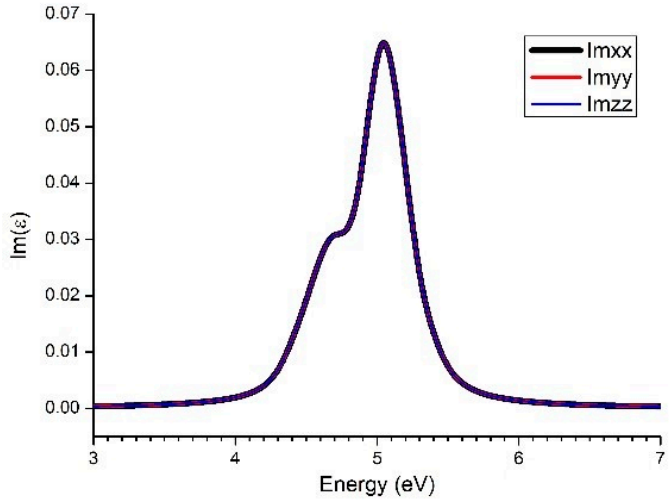

Figure 4. Imaginary part of dielectric function of pure YAG.

The imaginary part of the dielectric function of pure YAG obtained in this way, which directly gives the absorption spectra of YAG, is presented in Figure 4.

From the figure of research on the pure sample, we do not see any anisotropy.

The absorption edge starts from about 4.2 to 4.6 eV. The absorption spectrum consists of a very significant peak at 5 eV and also another peak structure at 4.7 eV. We can draw conclusions about the transparency of the sample in the visible region, because the absorption spectra appear in the UV region. Therefore, this system has weak absorption in the deep UV-VIS region (<250 nm), which depicts enough transparency for the routinely used lasers. This transparent nature makes them perfect candidates for deep UV nonlinear optical materials.

The real part of the dielectric function of the pure sample is plotted in Figure 5. The value of the static dielectric constant (value of dielectric function at zero energy) is 1.009.

From Figure 5, we can observe the anomalous dispersion region from 4.9 eV to 5.25 eV.

The refractive index value calculated from the relation [22] is equal to 1.005, in a spectral region 3–4 eV,

$$n^2 - k^2 = \mathrm{Im}(\varepsilon) \quad (5)$$

$$2nk = \mathrm{Re}(\varepsilon) \quad (6)$$

The maximum value is −1.014 at 4.3 eV, the minimum is 0.95 at 5.25 eV.

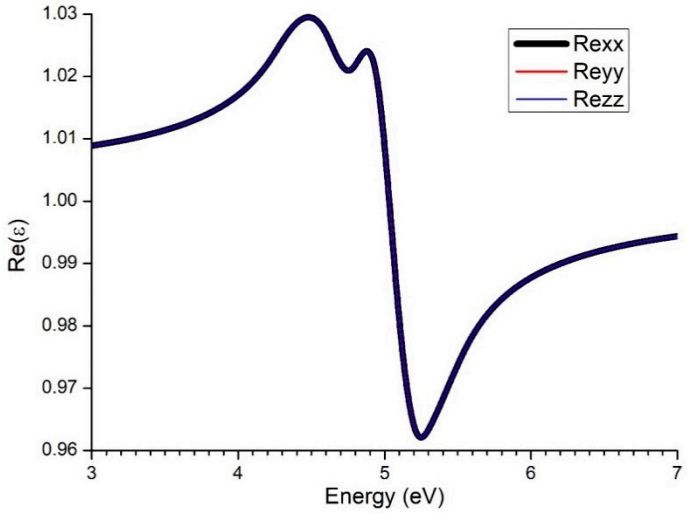

Figure 5. Real part of dielectric function.

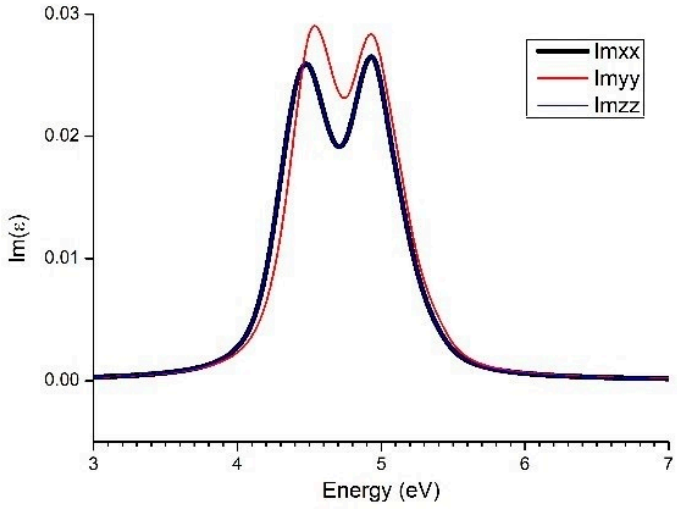

(**a**)

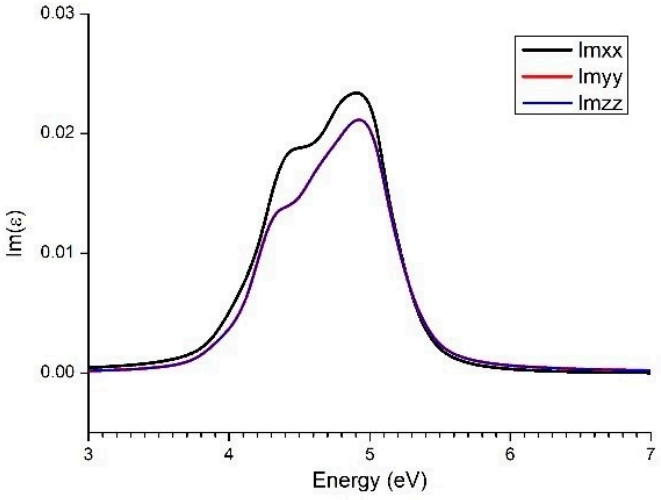

(**b**)

Figure 6. Imaginary part of dielectric function of YAG doped by La (**a**) with 2 atoms (**b**) with 4 atoms.

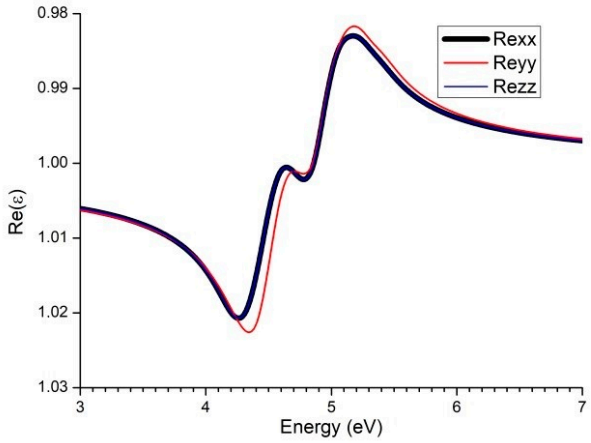

(**a**)

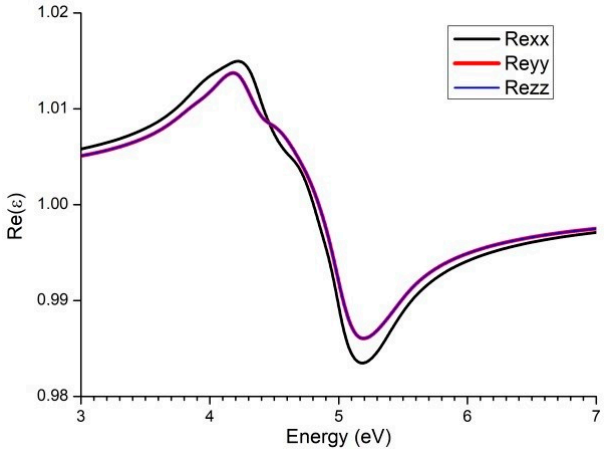

(**b**)

Figure 7. The real part of dielectric function in YAG doped by La (**a**) with 2 atoms (**b**) with 4 atoms.

3.2.2. Effect of Doping

We investigated the effect of doping on the optical properties of yttrium garnet.

One can notice the anisotropy in the optical properties along different axes when the sample is doped with lanthanum. Moreover, in the case of doping with two lanthanum atoms, the anisotropy is most pronounced along the *Y* axis, if doped by four atoms—along the *X* axis. It also depends on the position of the replaced atom, as shown in Figure 1. In the case of $Y_3Al_5O_{12}$:La (two ions), two peaks appear in region 4, 4 eV and 5 eV. There is a significant reduction in absorption coefficient in the region of energy of about 4.7 eV. In the case of $Y_3Al_5O_{12}$:La (four ions), indistinct and diffuse peaks are observed with lower values in the imaginary part of the permittivity around these energies.

As can be observed from Figures 4 and 6, absorption in the pure sample is two-times higher than in the doped one.

Therefore, the 5 eV peak in the pure sample, and 4.4 eV and 5 eV, is a main consideration for tailoring the optical properties of YAG in the visible range of light. Here, we can consider the appearance of a maximum at 4.4 eV when doping with two atoms of La.

The real part of the dielectric constant is presented in Figure 7.

The value of the static dielectric constant is about 1.006 in both samples. In the case of the second sample, the region of anomalous dispersion is noticeable from 4.2 eV to 5.2 eV.

4. Conclusions

In conclusion, the structural parameters, electronic structure and optical properties of pure YAG, one doped with two La ions and one with four La ions, were investigated by using the first principles within Quantum Expresso. Our structural parameters were slightly lower than the experimental values. From the analysis of the density of states, it is noted with an increase in the number of doped atoms, the DOS of the most populated levels of the host, decreases and DOS of the impurity atom increases and the position of the most populated levels shifts to the left in the region of negative energies in the case of two atoms and to the right in the case of four atoms. To discuss the optical properties, the dielectric function, absorption, refractive index, energy loss function and reflectivity were calculated. We can draw conclusions regarding the transparency of the sample in the visible region, because the absorption spectra appear in the UV region. It can be seen from the imaginary part of the dielectric function that, in the case of $Y_3Al_5O_{12}$:La (2 ions), two peaks appear in the region of 4.4 eV and 5 eV. Therefore, this system has weak absorption in the deep UV-VIS region (<250 nm), which depicts enough transparency for the routinely used lasers. This transparent nature makes them perfect candidates for deep UV nonlinear optical materials.

One peak in a pure sample, doped with four Lanthanum atoms, was registered. Anisotropy is most pronounced with an increase in the degree of doping. It is known that the large anisotropy in the refractive indices is a favorable factor for the appearance of phase-matching directions in the crystal, which are necessary for efficient conversion of laser radiation to the second harmonic. From the results obtained, it can be concluded that all the crystals under study are characterized by rather strong birefringence.

Author Contributions: Conceptualization, N.Z. and D.S.; methodology, Z.A.; software, D.S.; validation, A.Z. and K.B.; formal analysis, Z.A.; investigation, N.Z.; resources, D.S.; data curation, A.Z.; writing—original draft preparation, K.B.; writing—review and editing, N.Z.; visualization, Z.A.; supervision, N.Z.; project administration, A.Z. All authors have read and agreed to the published version of the manuscript.

Funding: This research was funded by the Ministry of Education and Science of the Republic of Kazakhstan by project No. AP09057946 "Spectroscopic studies of functional materials based on perovskites and garnets doped with Ln^{2+}, Ln^{3+}, Ln^{4+}".

Informed Consent Statement: Informed consent was obtained from all subjects involved in the study.

Conflicts of Interest: The authors declare no conflict of interest.

References

1. Weber, M.J. Optical spectra of Ce^{3+} and Ce^{3+}-sensitized fluorescence in $YAlO_3$. *J. Appl. Phys.* **1973**, *44*, 3205–3208. [CrossRef]
2. Zorenko, Y.; Gorbenko, V.; Voloshinovskii, A.; Vistovskii, V.; Nikl, M.; Mihokova, E.; Nejezchleb, K. Intrinsic and Ce^{3+}—Related Luminescence of Single Crystals and Single Crystalline Films of YAP Perovskites: New Results. *IEEE Trans. Nucl. Sci.* **2008**, *55*, 1186–1191. [CrossRef]
3. Setlur, A.A.; Happek, U. Cerium luminescence in nd0 perovskites. *J. Solid State Chem.* **2010**, *183*, 1127–1132. [CrossRef]
4. Sugak, D.; Matkovskii, A.; Savitskii, D.; Durygin, A.; Suchocki, A.; Zhydachevskii, Y.; Solskii, I.; Stefaniuk, I.; Wallrafen, F. Growth and induced color centers in $YAlO_3$–Nd single crystals. *Phys. Status Solidi A* **2001**, *184*, 239–250. [CrossRef]
5. Kaminskii, A.A. Laser crystals and ceramics: Recent advances. *Laser Photonics Rev.* **2007**, *1*, 93–177. [CrossRef]
6. Zhydachevskii, Y.; Durygin, A.; Suchocki, A.; Matkovskii, A.; Sugak, D.; Bilski, P.; Warchol, S. Mn-doped $YAlO_3$ crystal: A new potential TLD phosphor. *Nucl. Instrum. Methods Phys. Res. B* **2005**, *227*, 545–550. [CrossRef]
7. Zhydachevskii, Y.; Durygin, A.; Suchocki, A.; Matkovskii, A.; Sugak, D.; Loutts, G.B.; Noginov, M.A. Radiation and thermally induced effects in $YAlO_3$:Mn crystals. *J. Lumin.* **2004**, *109*, 39–49. [CrossRef]
8. Xia, Z.; Meijerink, A. Ce^{3+}-doped garnet phosphors: Composition modification, luminescence properties and applications. *Chem. Soc. Rev.* **2017**, *46*, 275–299. [CrossRef]
9. Chen, F.; Tan, Y.; Jaque, D. Ion-implanted optical channel waveguides in neodymium-doped yttrium aluminum garnet transparent ceramics for integrated laser generation. *Opt. Lett.* **2009**, *34*, 28–30. [CrossRef]
10. Jin, W.; Yin, W.; Yu, S.; Tang, M.; Xu, T.; Kang, B.; Huang, H. Microwave dielectric properties of pure YAG transparent ceramics. *Mater. Lett.* **2016**, *173*, 47–49. [CrossRef]

11. Ghrib, T.; Lafy, A.; Otaibi, A.; Abdullah Almessiere, M.; Ashahri, A.; Masoudi, I. Structural, optical and thermal properties of the Ce doped YAG synthesized by solid state reaction method. *Thermochim. Acta* **2017**, *654*, 35–39. [CrossRef]
12. Husnen, R.; Hassan, Z.; Ahmed, M.; Thahab, S.M.; Alsultany, H.; Omar, A.F. Ce-doped YAG single-crystals prepared by continuous wave (CW)–CO_2 laser combustion technique with attractive characteristics and moderate white LED performance. *Opt. Laser Technol.* **2020**, *132*, 106506.
13. Feng, S.; Qin, H.; Wu, G.; Jiang, H.; Zhao, J.; Liu, Y.; Luo, Z.; Qiao, J.; Jiang, J. Spectrum regulation of YAG:Ce transparent ceramics with Pr, Cr doping for white light emitting diodes application. *J. Eur. Ceram. Soc.* **2017**, *37*, 3403–3409. [CrossRef]
14. Zorenko, Y.; Gorbenko, V.; Voznyak, T.; Zorenko, T.; Nikl, M.; Nejezchleb, K. Luminescence of La^{3+} and Sc^{3+} impurity centers in $YAlO_3$ single-crystalline films. *J. Lumin.* **2008**, *128*, 595–602. [CrossRef]
15. Zorenko, Y.; Gorbenko, V.; Zorenko, T.; Voznyak, T.; Voloshynovskii, A.; Vistovskiy, V.; Paprocki, K.; Mosińska, L.; Bilski, P.; Twardak, A.; et al. Luminescent and scintillation properties of Sc^{3+} and La^{3+} doped Y_2SiO_5 powders and single crystalline films. *J. Lumin.* **2016**, *179*, 445–450. [CrossRef]
16. Khaliq, F.; Ayub, K.; Mahmood, T.; Muhammad, S.; Tabassum, S.; Gilani, M.A. First example of lanthanum as dopant on $Al_{12}N_{12}$ and $Al_{12}P_{12}$ nanocages for improved electronic and nonlinear optical properties with high stability. *Mater. Sci. Semicond. Process.* **2021**, *135*, 106122. [CrossRef]
17. Zvonarev, S.V.; Churkin, V.Y.; Pankov, V.A.; Chesnokov, K.Y.; Chukin, A.V.; Abramov, A.V. Luminescence of alumina ceramic doped with lanthanum under medium- and high-dose irradiation. *Nucl. Inst. Methods Phys. Res. B* **2020**, *465*, 42–46. [CrossRef]
18. Kar, B.S.; Goswami, M.; Jana, P. Effects of lanthanum dopants on dielectric and multiferroic properties of $BiFeO_3$–$BaTiO_3$ ceramics. *J. Alloys Compd.* **2020**, *861*, 157960. [CrossRef]
19. Chakrabarti, C.; Fu, Q.; Chen, X.; Qiu, Y.; Yuana, S.; Li, C. Modulation of magnetic, ferroelectric and leakage properties by $HoFeO_3$ substitution in multiferroic $0.7BiFeO_3$-$0.3Ba_{0.8}Ca_{0.2}TiO_3$ solid solutions. *Ceram. Int.* **2020**, *46*, 212–217. [CrossRef]
20. Zhou, W.; Zheng, Q.; Li, Y.; Li, Q.; Wan, Y.; Wu, M.; Lin, D. Structure, ferroelectric, ferromagnetic and piezoelectric properties of Al-modified $BiFeO_3$–$BaTiO_3$ multiferroic ceramics. *Phys. Status Solidi A* **2015**, *212*, 632–639. [CrossRef]
21. Zhu, J.; Sidletskiy, O.; Boyaryntseva, Y.; Grynyov, B. Structure and role of carbon-related defects in yttrium aluminum garnet. *Opt. Mater.* **2021**, *111*, 110561. [CrossRef]
22. Gracia, J.; Seijo, L.; Barandiarán, Z.; Curulla, D.; Niemansverdriet, H.; Gennip, N. Ab initio calculations on the local structure and the 4f–5d absorption and emission spectra of Ce^{3+}-doped YAG. *J. Lumin.* **2008**, *128*, 1248–1254. [CrossRef]
23. Chen, L.; Chen, X.; Liu, F.; Chen, H.; Wang, H.; Zhao, E.; Jiang, Y.; Chan, T.-S.; Wang, C.-H.; Zhang, W.; et al. Charge deformation and orbital hybridization: Intrinsic mechanisms on tunable chromaticity of $Y_3Al_5O_{12}$:Ce^{3+} luminescence by doping Gd^{3+} for warm white LEDs. *Sci. Rep.* **2015**, *5*, 11514. [CrossRef] [PubMed]
24. Ronda, C.; Wieczorek, H.; Khanin, V.; Rodnyi, P. Review-scintillators for medical imaging: A tutorial overview. *ECS J. Solid State Sci. Technol.* **2016**, *5*, 3121–3125. [CrossRef]
25. Zitouni, H.; Tahiri, N.; El Bounagui, O.; Ez-Zahraouy, H. Doping effect of iodine on electronic and optical properties of perovskite $CsPbBr_3$ compound for photovoltaic applications: Ab initio calculations. *J. Electron. Spectrosc. Relat. Phenom.* **2021**, *247*, 147043. [CrossRef]
26. Dale Kleppinger, D.; Lindholm, F. Impurity concentration dependent density of states and resulting fermi level for silicon. *Solid-State Electron.* **1971**, *14*, 407–416. [CrossRef]